

# The biomechanics of fast prey capture in aquatic bladderworts

Amit K. Singh, Sunil Prabhakar  
 and Sanjay P. Sane\*

National Centre for Biological Sciences, Tata Institute of Fundamental Research, Bangalore 560065, India

\*Author for correspondence (sane@ncbs.res.in).

**Carnivorous plants match their animal prey for speed of movements and hence offer fascinating insights into the evolution of fast movements in plants. Here, we describe the mechanics of prey capture in aquatic bladderworts *Utricularia stellaris*, which prey on swimming insect larvae or nematodes to supplement their nitrogen intake. The closed *Utricularia* bladder develops lower-than-ambient internal pressures by pumping out water from the bladder and thus setting up an elastic instability in bladder walls. When the external sensory trigger hairs on their trapdoor are mechanically stimulated by moving prey, the trapdoor opens within 300–700  $\mu$ s, causing strong inward flows that trap their prey. The opening time of the bladder trapdoor is faster than any recorded motion in carnivorous plants. Thus, *Utricularia* have evolved a unique biomechanical system to gain an advantage over their animal prey.**

**Keywords:** carnivorous plants; *Utricularia*; high-speed videography

## 1. INTRODUCTION

Actively carnivorous plants offer fascinating insights into the selective pressures that drive the evolution of novel, non-neural mechanisms to generate rapid movements [1]. These fast movements are typically driven by mechanical instabilities involving sudden release of stored energy or explosive fracture of the tissue. The speed of such movements depends on the geometry and material architecture of the plant tissues, as well as the length scales over which these movements occur [2,3].

Slower plant movements, as in case of the touch-sensitive tropical weed, *Mimosa pudica*, are associated with swelling or shrinking of plant cells owing to transport of water within it and require over tens of seconds for full actuation [4,5]. By contrast, faster hydraulic movements (approximately tens of milliseconds) in many plants occur via two forms of elastic instabilities in the pre-stressed tissue. First, as in the case of Venus flytraps (*Dionaea muscipula*), rapid structural changes may be actuated by a sudden (or snap) buckling of a thin pre-stressed tissue [6]. Second, as in the case of rapid seed dispersal process in the sandbox tree *Hura crepitans* [7], or spore dispersal in many fungi [8],

a fast propagating fracture in the pre-stressed tissue causes it to tear in very short timescales (approximately a few milliseconds). Because the latter processes are irreversible, they cannot be used by plants for regular activities such as feeding.

Despite these physical constraints, many plants have evolved mechanisms that enable rapid movements. Here, we use a combination of high-speed videography, pressure measurements and flow visualization to investigate the prey capture mechanism of aquatic bladderworts of the genus *Utricularia*. These plants free-float in water and have evolved a carnivorous life-style to supplement their nitrogen intake. Each prey capture unit of *U. stellaris* is a modified leaf structure in the shape of a bladder equipped with a trapdoor (figure 1*a,b*; see also [9]). The closed bladder pumps out water, which combined with outward recoil of its bladder walls causes lower-than-ambient internal pressure [10,11]. When the trigger hairs are stimulated by mechanical activation, the trapdoor opens causing a sudden influx of water driven by this pressure differential. These flows can capture smaller animals within the bladder or suction-tether prey several times larger than the bladders. After capturing prey, the trapdoor rapidly closes to engulf the prey. This enables bladderworts to outpace sensorimotor timescales, and offers them an advantage over their animal prey.

## 2. MATERIAL AND METHODS

*Utricularia stellaris* are aquatic bladderworts widely distributed throughout South Asia, Japan and Australia [12]. These plants were readily collected from local perennial lakes in Bangalore and cultivated in smaller outdoor water containers. The bladders remained healthy under these conditions, as evident from the fact that the plants regularly produced flowers.

### (a) High-speed videography of *Utricularia stellaris* trapdoor kinematics

Before filming, fresh bladders (bladder length approx. 2 mm, trapdoor approx. 0.8 mm, internal volume approx. 1.5  $\mu$ l) were transferred to transparent plastic Petri dishes. We activated the trapdoors by gently touching their trigger hairs with a microcapillary tip. We backlit the traps with 90 W fluorescent lights and filmed the opening-closing kinematics of trapdoors at 15 000 frames  $s^{-1}$  using a high-speed video camera (exposure time = 64.5  $\mu$ s, 512  $\times$  384 pixel resolution; Phantom v. 7.3, Vision Research Inc.).

### (b) Measurement of the pressure inside the *Utricularia* bladder

To measure the pressure difference across bladder walls, we used a method described in Green & Stanton [13]. A graduated glass microcapillary (internal diameter of 280  $\mu$ m and drawn to a 20  $\mu$ m tip) was filled with water, leaving behind a tiny air bubble inside, while the other end of the capillary tube was sealed. We calibrated this microprobe by inserting it to various known depths of water, while monitoring the bubble size as a function of the hydraulic pressure at that depth. Using this calibration procedure, we determined the pressure inside the bubble  $P_0$  (which includes capillary pressure) to be approximately 55 kPa. The calibration procedure also showed that ideal gas laws hold for volumetric changes in the microprobe bubble (see the electronic supplementary materials for details).

This calibrated microprobe was then mounted to a single axis micromanipulator (MM-3, Narishige Scientific) for pressure measurements. The open end of the pressure microprobe was inserted into the bladder wall. The small size of the microprobe tip ensured that its insertion does not cause rending in, or leakage across, the bladder wall; capillary and closed bladder formed a closed system whose internal pressure could be monitored. When the microprobe was inserted into the bladder containing lower-than-ambient internal pressure, the inner meniscus of the microprobe bubble moved towards the tip, causing an increase in the bubble size. Because ideal gas laws appear to hold true for the microcapillary air bubble, the equilibrium

Electronic supplementary material is available at <http://dx.doi.org/10.1098/rsbl.2011.0057> or via <http://rsbl.royalsocietypublishing.org>.

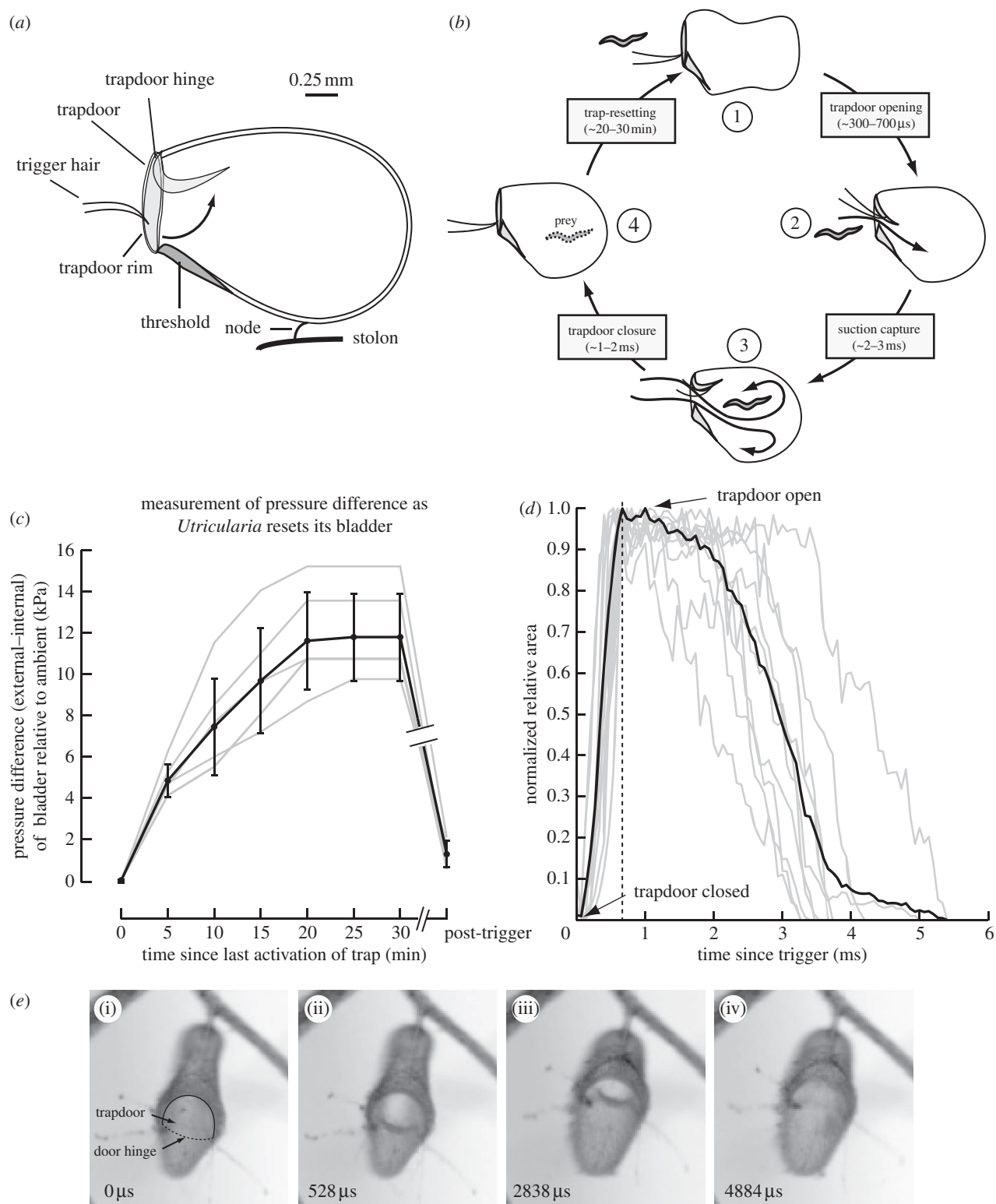


Figure 1. Opening and closing of the trapdoor of *U. stellaris* and related flows. (a) Diagram of *U. stellaris* bladder. Arrow shows opening of the trapdoor. (b) Summary of prey capture in *U. stellaris* including timescales measured in this study. Following an unsuccessful capture, the trap resets in approximately 20–30 min (1). When the trigger hairs are mechanically stimulated by prey, the trap door opens in 300–700  $\mu\text{s}$  (2) to generate strong suction flows that capture (3) and digest (4) prey. (c) *Trap-resetting phase*. Plot shows how the closed bladder generates lower than ambient internal pressures. The  $x$ -axis indicates time elapsed since the last successful activation of the trapdoor and the  $y$ -axis indicates the external (higher)–internal (lower) pressure of the bladder. The break in axis and plots indicates post-stabilization of internal pressure, the trap can be retriggered after any arbitrary time duration to rapidly bring it back to zero state. (d) *Opening and closing kinematics of the trapdoor*. Trapdoor kinematics is depicted as a ratio of area of the open mouth to a reference rim area with time. Grey lines show 10 individual plots normalized to maximum ratio of areas (for a fully open trap), the dark black line shows the normalized average curve of these 10 plots. The dashed black line shows the average time point of bladder opening. (e) *Opening and closing phase*. Four frames from a video capture show *U. stellaris* trapdoor in the following stages: (i) initiation of opening, (ii) fully open, (iii) before closing, and (iv) fully closed. Numbers in the lower left corner of each figure indicate time (microseconds) elapsed since initiation of door opening. The door hinge (dotted line) and margin (continuous) are labelled in panel (i). Typical diameter of the trap door is 0.8 mm.

pressure inside the bladder ( $P_{\text{bladder}}$ ) is

$$P_{\text{bladder}} = P_0 \frac{V_0}{V_{\text{bladder}}}. \quad (2.1)$$

From these measurements, we calculated the pressure difference ( $\Delta P = P_{\text{bladder}} - P_0$ ) across the bladder walls.

Next, we measured the changes in the internal pressure of the bladder relative to ambient by monitoring changes in the bubble size every 5 min, each time stimulating the trigger hair (figure 1c). The trapdoor did not activate until the internal pressure was sufficiently lower than ambient, suggesting a refractory period immediately post-trigger. Upon firing, the relative internal pressure resets to zero. Although this method reliably measures equilibrium pressures of the bladder, it cannot capture fast dynamical changes in internal pressure owing to the equilibration time for bubble pressure in the microprobe.

### (c) Measurement of trapdoor kinematics

Because unrestricted traps swivel substantially during opening, it was difficult to track the absolute areas of the trapdoors. Instead, we quantified the kinematics of opening and closing of trapdoors as a ratio of the open to reference area, which move together keeping their ratio constant. Individual frames from the high-speed video were analysed using a custom MATLAB (Mathworks Inc., Natick, MA, USA) code to determine pixel areas of open and reference areas. We validated this method using printed images of two concentric circles with known ratio of areas using images taken from arbitrary angles. For each bladder, the ratio of open and reference areas was normalized by assigning a value of 1 to the maximum ratio (fully open door) and 0 to minimum value of the ratio (fully closed door; figure 1d). This method ensured that final plots remained independent of absolute trapdoor sizes.

### (d) Estimation of flows

We placed several small epichlorophydrin-dextran beads (diameter = 80–100  $\mu\text{m}$ ) coated with methylene blue near the bladder mouth. The bladder was held against a calibration grid (0.25 mm markings) using wax to restrict its swivelling movement around its node. The movement of the beads was recorded using high-speed cameras and digitized using MATLAB.

For a system driven by pressure difference alone, the Navier–Stokes equation may be simplified from its Eulerian form:

$$\frac{Du}{D\tau} = -\frac{\nabla P}{\rho}, \quad (2.2)$$

to

$$\Delta u = -\frac{\partial P}{\rho \partial x} \Delta \tau, \quad (2.3)$$

where  $u$  is the flow velocity,  $\partial P$  the pressure differential across the bladder wall,  $\rho$  the density of water, and  $\partial x$  and  $\Delta \tau$  the length scale of flows and timescale of the lid opening, respectively.

Using experimentally measured values ( $\partial P = -11\,800$  Pa,  $\rho = 1000$  kg m $^{-3}$ ,  $\partial x = 2 \times 10^{-3}$  m and  $\Delta \tau = 4 \times 10^{-4}$  s) in equation (2.3) provides a flow estimate of 2.4 m s $^{-1}$ , in close agreement with our influx measurements. Thus, flows were largely driven by the pressure differential between the inside and outside of the bladder.

## 3. RESULTS AND DISCUSSION

At equilibrium, the quiescent *U. stellaris* bladder actively transports water out by a mechanism that derives its energy from respiration [10,11], causing its walls to become inwardly concave. The elastic recoil tendency of the bladder wall balances the lower-than-ambient internal pressure to set up a mechanosensitive trigger.

Using the pressure measurement technique described above, we monitored the slow decrease in internal pressures in the bladder immediately following trigger, by monitoring the slow increase in the size of an enclosed air bubble within the graduated microprobe. The difference between external and internal pressures increased from 0 kPa ( $n = 6$ ) to a steady-state value of 11.8 kPa (s.d. =  $\pm 2.11$ ,  $n = 6$ ) over a

period of 20–30 min (figure 1c), in agreement with earlier measurements [14,15]. During resetting, the bladder was refractory and its trigger hairs were inactive. This indicates that an internal sensing mechanism allows the trigger to activate only beyond a threshold pressure difference. When sufficient pressure difference was generated, the trap could be activated by touching the mechanosensitive trigger hairs on the outer lip of the bladder. The exact mechanism leading from transduction to opening is presently unknown.

Mechanical stimulation of the trigger hair on the trapdoor caused it to open rapidly within 300–700  $\mu\text{s}$  ( $n = 10$ ; figure 1d,e) resulting in suction of the surrounding water into the bladder. After remaining open for 1–3 ms, the bladder closed over a period of 1–2 ms (figure 1d,e). To the best of our knowledge, these are the fastest movements yet reported in carnivorous plants. We tracked the motion of neutrally buoyant coloured beads engulfed into the trap to measure the rapid suction flow-speeds generated by opening of the trapdoor. Near the door, the flow velocities were maximum with a value of 2.7 m s $^{-1}$  (s.d. = 0.2 m s $^{-1}$ , eight beads, four videos) and of the same order of magnitude as theoretically estimated from flows (approx. 2.4 m s $^{-1}$ ) that are primarily driven by the pressure differential across the bladder. Based on the bladder dimensions of approximately 1 mm, velocity of flow approximately 2.4 m s $^{-1}$  and kinematic viscosity of water at 20°C of approximately 10 $^{-6}$  m $^2$  s $^{-1}$ , we calculate the Reynolds number to be in the range of 2400. Thus, the suction flows that develop within 1–3 ms following door opening are strongly inertial and capture smaller prey. We hypothesize that because their timescales outpace the typical durations of sensorimotor responses, it is difficult for prey to detect the sudden flow. Moreover, the bladder can reorient around the flexible node and effectively suction-tether larger prey. If unsuccessful, however, the bladder resets in 20–30 min for another capture.

In conclusion, although studied extensively [9,16–18], the bladderworts trapdoor kinematics are too fast to be captured by previous methods resulting in gross underestimation of their timescales by an order of magnitude. Like other rapid movements at these lengths (approx. 2 mm) and timescales (approx. 10 $^{-4}$  s), opening of the *Utricularia* trapdoor may be dictated by mechanical instabilities in bladder walls [3] and fluid influx is driven by the pressure difference across bladder walls. These mechanisms enable *Utricularia* traps to successfully match their animal prey for speed of movement.

We thank R. Jacob, N. Saxena, H. Bhat, P. Pullarkat and M. K. Mathew for invaluable feedback and the Asian Office for Aerospace Research and Development (AOARD) for funding.

- 1 Juniper, B. E., Robins, R. J. & Joel, D. M. 1989 *The carnivorous plants*. London, UK: The Academic Press.
- 2 Dumais, J. 2007 Can mechanics control pattern formation in plants? *Curr. Opin. Plant Biol.* **10**, 58–62. (doi:10.1016/j.pbi.2006.11.014)
- 3 Skotheim, J. M. & Mahadevan, L. 2005 Physical limits and design principles for plant and fungal movements. *Science* **308**, 1308–1310. (doi:10.1126/science.1107976)

- 4 Hill, B. S. & Findlay, G. P. 1981 The power of movement in plants: the role of osmotic machines. *Q. Rev. Biophys.* **14**, 173–222. (doi:10.1017/S003358350002249)
- 5 Robert, D. A. 1969 Mechanism of the seismonastic reaction in *Mimosa pudica*. *Plant Physiol.* **44**, 1101–1107. (doi:10.1104/pp.44.8.1101)
- 6 Forterre, Y., Skotheim, J. M., Dumais, J. & Mahadevan, L. 2005 How the Venus flytrap snaps. *Nature* **433**, 421–425. (doi:10.1038/nature03185)
- 7 Swaine, M. D. & Beer, T. 1977 Explosive seed dispersal in *Hura crepitans* L. (Euphorbiaceae). *New Phytol.* **78**, 695–708. (doi:10.1111/j.1469-8137.1977.tb02174.x)
- 8 Page, R. M. 1964 Sporangium discharge in *Pilobus*: a photographic study. *Science* **146**, 925–927. (doi:10.1126/science.146.3646.925)
- 9 Lloyd, F. E. 1935 *Utricularia*. *Biol. Rev. Camb. Phil. Soc.* **10**, 72–110. (doi:10.1111/j.1469-185X.1935.tb00477.x)
- 10 Sydenham, P. H. & Findlay, G. P. 1973 Rapid movement of bladder of *Utricularia* sp. *Aust. J. Biol. Sci.* **26**, 1115–1126.
- 11 Sydenham, P. H. & Findlay, G. P. 1975 Transport of solutes and water by resetting bladders of *Utricularia*. *Aust. J. Plant Physiol.* **2**, 335–351. (doi:10.1071/PP9750335)
- 12 Janarthanam, M. K. & Henry, A. N. 1992 *Bladder worts of India*. Calcutta, India: Botanical Survey of India.
- 13 Green, P. B. & Stanton, F. W. 1967 Turgor pressure: direct manometric measurement in single cells of *Nitella*. *Science* **155**, 1675–1676. (doi:10.1126/science.155.3770.1675)
- 14 Sasago, A. & Sibaoka, T. 1985 Water extrusion in the trap bladders of *Utricularia vulgaris*. I. A possible pathway of water across the bladder wall. *Bot. Mag. Tokyo* **98**, 55–66. (doi:10.1007/BF02488906)
- 15 Sasago, A. & Sibaoka, T. 1985 Water extrusion in the trap bladders of *Utricularia vulgaris*. II. A possible mechanism of water outflow. *Bot. Mag. Tokyo* **98**, 113–124. (doi:10.1007/BF02488791)
- 16 Cohn, F. 1875 Ueber die function der blasen von *Aldrovanda* und *Utricularia*. *Cohn's Beitrage zur Biologie der Pflanzen* **1**, 71–95.
- 17 Darwin, C. 1875 *Insectivorous plants*. New York, NY: D Appleton and Company.
- 18 Skutch, A. 1928 The capture of prey by the bladderwort. *New Phytol.* **27**, 261–297. (doi:10.1111/j.1469-8137.1928.tb06742.x)